Figure S1. Flow cytometry data of HeLa S3 cells harvested at different phases.

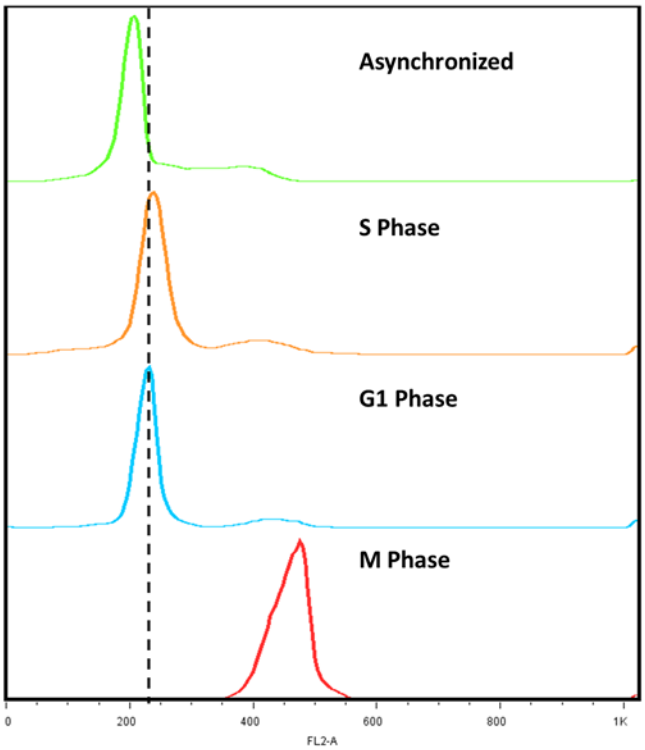

Figure S2. RP-HPLC purification of acid-extracted histone mixtures of asynchronized HeLa S3 cells. Histone H3.1 was well separated from H3.2 and H3.3.

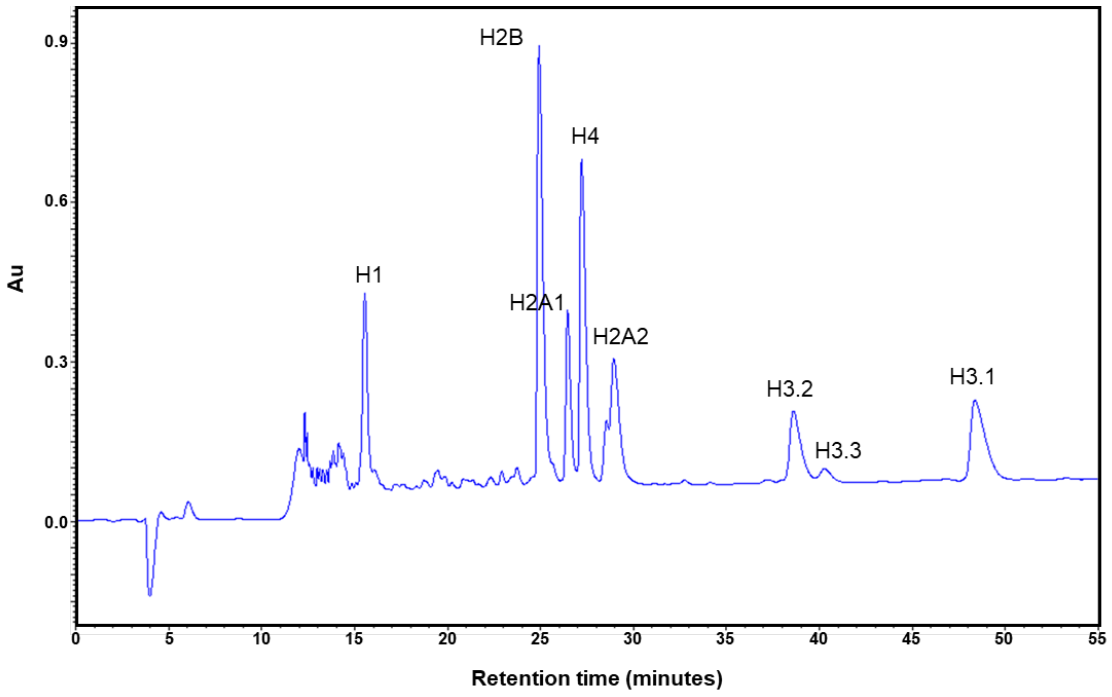

Figure S3. Representative ETD product ion spectrum for the deconvoluted spectrum of (A) K9me2S10phK23acK27ac and (B) K9me2S10phT11ph.

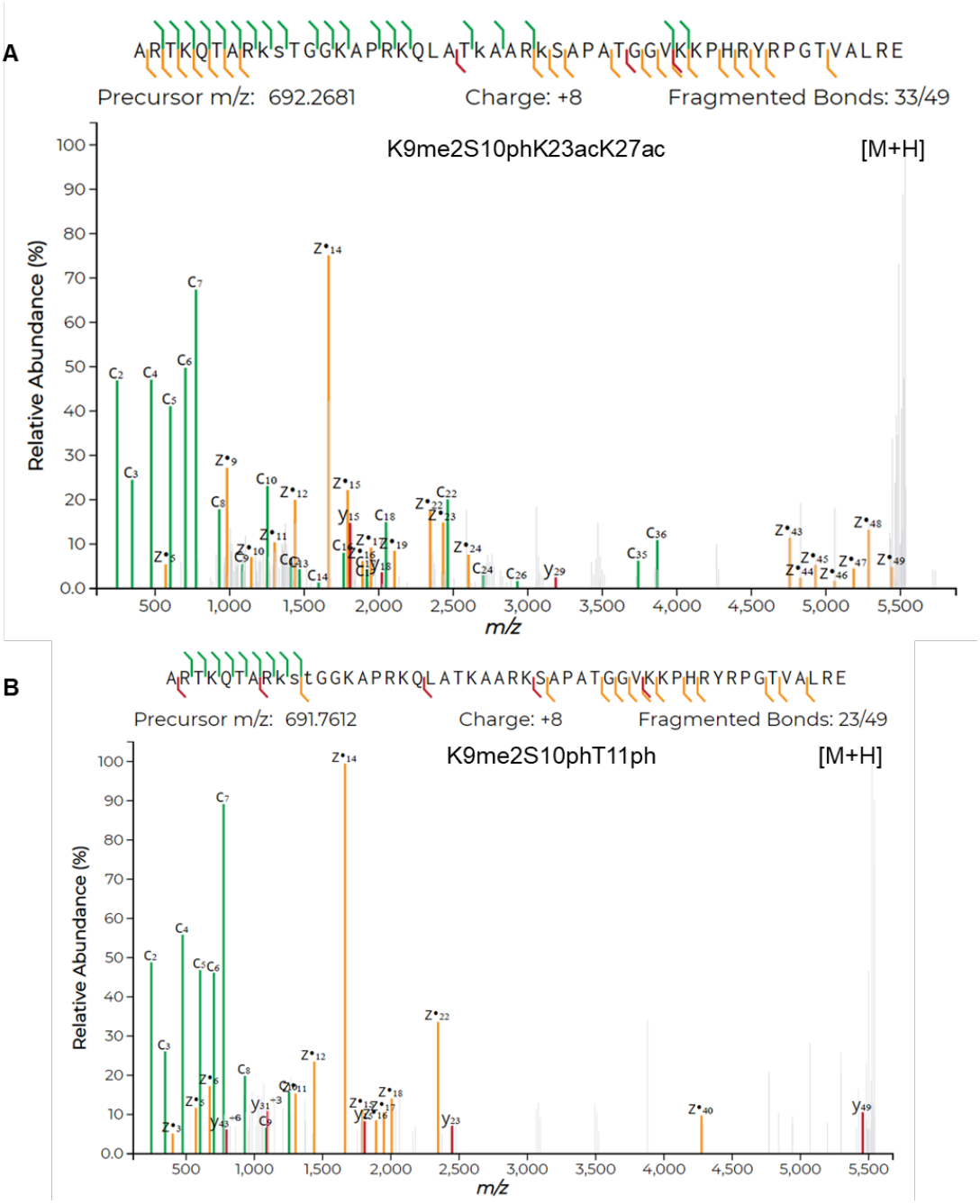

Figure S4. Characterization of histone code. (A) Number of detected histone codes in each sample. (B) Sum of the counts of histone codes based on the detected frequency. (C) Sum of the relative abundance of histone codes based on the detected frequency.

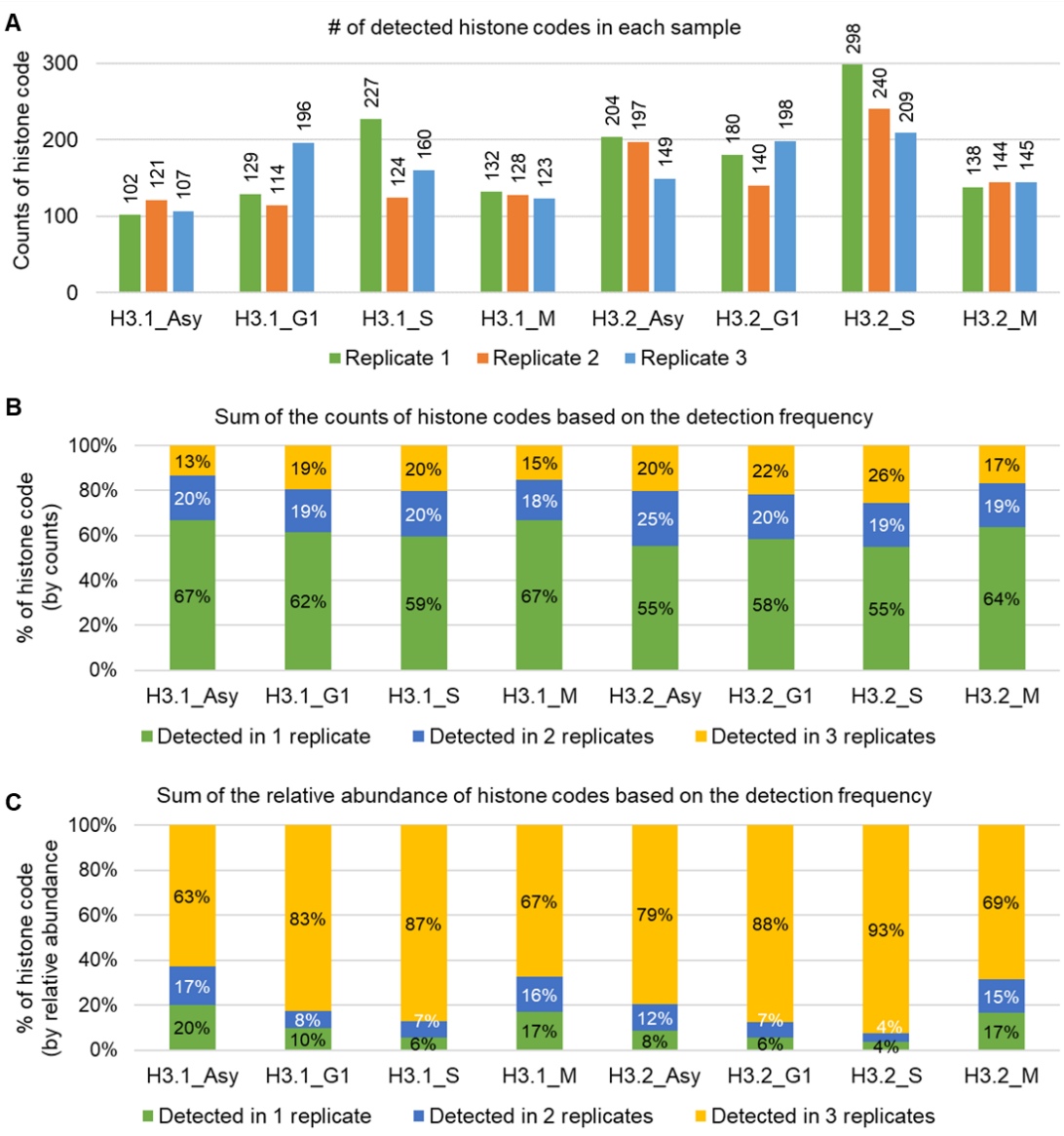

Figure S5. (A) Bar graph of relative abundance for K9me2 and K27me3 on histone H3. Average ± standard deviation of three replicates. (B) WB results of anti-H3K9me2 and anti-H3K27me3 in distinct phases.

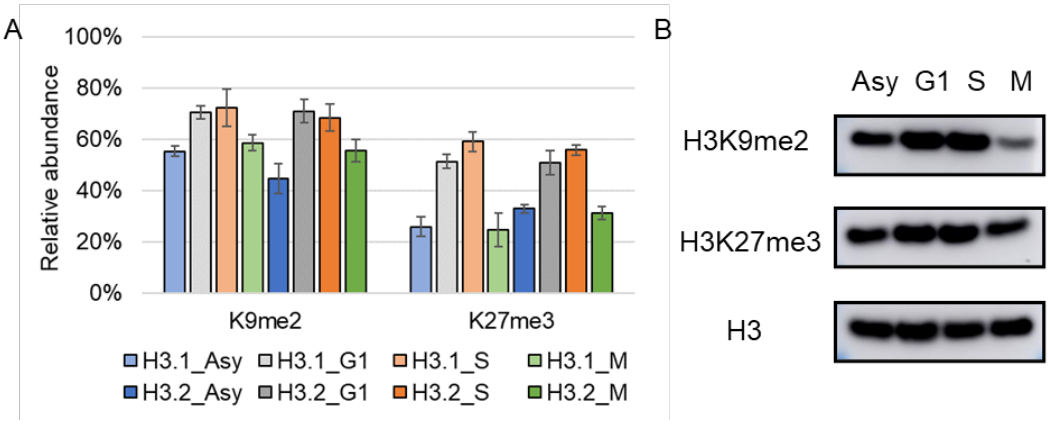

Figure S6. Volcano plots of single marks relative abundance for H3.1/H3.2 in (A) asynchronized HeLa S3 cells and cells synchronized in (B) G1 phase, (C) S phase and (D) M phase.

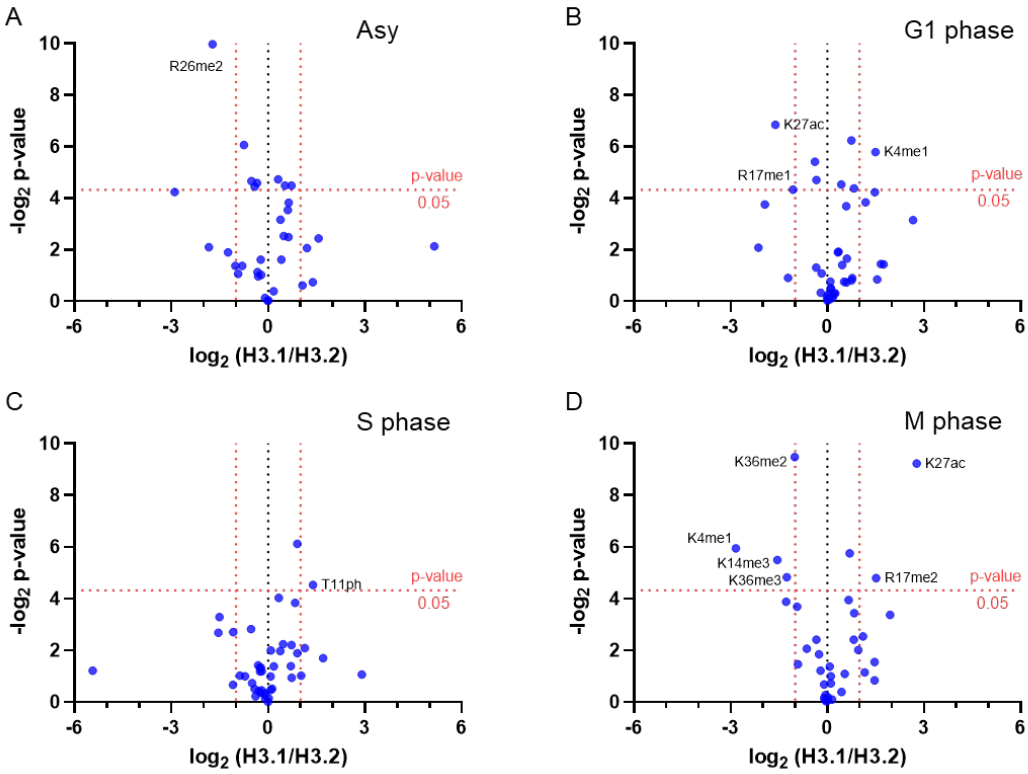

Figure S7. Pearson correlation coefficient matrix heatmap of different phases by investigating H3 single mark relative abundance (the upper-right corner), and binary mark relative abundance (the lower-left corner).